Beyond BMI: Validating iBMI and dBMI to define novel obesity clusters and stratify metabolic risk.

Running title: iBMI and dBMI: Novel Tools for Obesity Clustering and Risk Stratification

Authors:

Dr. Suresh N. Shinde, MD, MNAMS

Dr. Rituparna S. Shinde, MD, DNB (Cardiology)

Dr. Succhietra Y. Bhangaaley, BHMS, CCR

Affiliations:

Academy of Continuing Medical Education & Research, Pune, India

Poona Hospital & Research Center, Pune, India

Correspondence:

Dr. Suresh N. Shinde (acmepune@yahoo.com)

Beyond BMI: Validating iBMI and dBMI to define novel obesity clusters and stratify metabolic risk.

Abstract

Background

Conventional Body Mass Index (BMI) fails to account for fat distribution and often misclassifies metabolic risk, particularly in South Asian populations with higher visceral adiposity at lower BMI thresholds. We aimed to develop improved anthropometric indices that integrate waist circumference and height to better reflect central adiposity and metabolic risk.

Methods

In this retrospective observational study at a metabolic clinic in India, we analyzed clinical and anthropometric data from 331 adults. We introduced the Improvised BMI (iBMI = Weight * WC / Height) and derived the Delta BMI (dBMI = [iBMI minus BMI] / Height) as a height adjusted proxy for visceral adiposity. A subset of 67 participants underwent DEXA based body composition analysis. We used clustering, regression modeling, and ROC analysis to compare iBMI, dBMI, and the graphical metric, Graphical Risk Distance (GRD), with established metabolic markers including HOMA1IR, fasting insulin, and DEXA derived visceral fat.

Results

Three metabolic phenotypes were identified through unsupervised clustering. In the non-diabetic subgroup (n=208), dBMI showed strong correlation with insulin resistance (AUC = 0.81), comparable to FPI (1.0), HOMA B (0.89), and DEXA.VAT (0.71). GRD and dBMI were also strongly correlated ($R^2 = 0.436$). The iBMI/BMI nomogram enabled visual stratification based on GRD, with predefined risk zones. iBMI classification thresholds derived from GRD intercepts were proposed to define underweight (<26), normal (26 to 35), overweight (36 to 40), and Obesity Classes I to III (>40), facilitating clinical interpretability.

Conclusions

The novel indices iBMI, dBMI, and GRD represent scalable, physiology based tools for early identification of visceral adiposity and insulin resistance. Their integration into routine anthropometric screening may enhance metabolic risk stratification, particularly in low resource or preclinical settings.

Beyond BMI: Validating iBMI and dBMI to define novel obesity clusters and stratify metabolic risk.

Introduction

Body mass index (BMI), introduced by Adolphe Quetelet in the 19th century, remains the global standard for assessing overweight and obesity. Defined as weight (kg) divided by height squared (m^2), BMI is widely used due to its simplicity and utility in clinical and epidemiological contexts. However, it fails to account for fat distribution—particularly central adiposity—which is more strongly linked to insulin resistance, type 2 diabetes, and cardiovascular disease than overall weight.

The limitations of BMI have been well documented. Yajnik and Yudkin (2004) demonstrated that individuals with similar BMI values across different ethnicities may have markedly divergent fat distributions and metabolic risks. The Multi-Ethnic Study of Atherosclerosis (MESA, 2014) confirmed that visceral fat, rather than BMI, is the dominant predictor of cardiometabolic risk across age, sex, and racial groups. Furthermore, the 'height-squared' denominator in BMI formula introduces geometric distortions, often necessitating ethnicity-specific thresholds, particularly for Asian populations, which are prone to metabolic complications at lower BMI levels.

Recognizing the human torso as being more cylindrical than planar, we propose an improved anthropometric metric, improvised Body Mass Index (iBMI), defined as:
iBMI (kg·m/m) = [Weight (kg) × Waist Circumference (m)] / Height (m)
This formulation incorporates waist circumference (WC) as a direct surrogate for abdominal adiposity, eliminates the need for height-squared scaling, and offers a more physiologically congruent construct. Compared to BMI, iBMI typically yields higher absolute values under normal conditions, a difference we term the *basal gap*. However, this gap is not uniform; it is modulated by individual height, which influences both the baseline offset and the slope of the iBMI–BMI relationship.

To normalize this variation and extract a height-independent risk signal, we derive the differential index (dBMI) as: dBMI = (iBMI – BMI) / Height (in meters)
We hypothesize that positive deviations in dBMI primarily reflect excess visceral adiposity, while negative or neutral values may indicate peripheral muscular mass (e.g., gluteal or deltoid bulk) or low-risk fat distribution patterns. This scaling also enhances comparability across body types and ethnicities, potentially correcting false BMI elevations in athletes and underestimations in short-stature individuals.

In this study, we evaluate iBMI as a waist-based index of central adiposity and assess its correlation with key metabolic parameters including fasting plasma glucose (FPG), glycated hemoglobin (HbA1c), HOMA1-B, and visceral fat by BEA and DEXA as well. We also validate the risk relevance of the newly defined dBMI and develop a clinically intuitive nomogram for early vascular risk stratification. This height-adjusted metric amplifies the signal of central adiposity and yields a dimensionally appropriate value reflective of metabolic risk burden.

Methods

This was a physician-led, non-interventional, retrospective chart-based observational study conducted at a metabolic clinic in India. Clinical records of 331 adult patients who visited for routine consultations over a one-year period were analyzed. All participants had previously provided written informed consent, and data were anonymized prior to analysis.

Anthropometry and Biochemistry:
Weight (kg), height (cm), and waist circumference (WC, cm) were recorded for each subject. From these, the following indices were computed:
• BMI (kg/m^2) = Weight / $Height^2$
• iBMI (kg·m/m) = (Weight * WC) / Height

Visceral fat percentage was estimated using the Omron KaradaScan HBF-375 Body Composition Monitor, a widely available, very low-cost bioelectrical impedance analyzer. This device reports visceral fat levels on a unitless scale from 0.5 to 30, with 30 representing the upper measurable limit. A subset of 67 participants also underwent body composition analysis using the GE Lunar Prodigy Dual-Energy X-ray Absorptiometry (DEXA) system. In addition to quantifying total fat mass and lean mass, the device's CoreScan™ application was employed to estimate visceral adipose tissue (VAT) mass in grams. CoreScan utilizes a proprietary algorithm that derives VAT measurements from total body DXA scans, offering a reliable, low-radiation alternative to CT or MRI. Blood samples were analyzed for fasting plasma glucose (FPG), fasting plasma insulin (FPI), and glycated hemoglobin (HbA1c) using standard biochemical and ELISA-based methods. HOMA1-IR and HOMA1-B were calculated using established formulae.

Clustering and Visualization:
To explore distinct metabolic phenotypes, K-means clustering (k=3) was applied using FPG, FPI, and BEA Visceral Fat data. Principal Component Analysis (PCA) was performed for dimensionality reduction and visual representation of the clusters (Figure 1), which delineated three metabolic groups: healthy, intermediate, and unhealthy.

A non-diabetic subgroup (n=208) was selected from the total 331 subjects, by excluding those with FPG >125 mg/dL or HbA1c >6.4%, to focus on early metabolic deviations. A scatter plot of iBMI vs. BMI was generated for this subgroup (Figure 2A), with a linear regression line fitted through the data points. This regression line was conceptualized as the adipose tissue Equipoise Line (EPL), representing a physiologic balance between subcutaneous (SAT) and visceral adipose tissue (VAT). Deviation from the EPL was theorized to reflect VAT predominance (i.e. WC-driven rise in iBMI not compensated by height). This led to the derivation of a novel metric termed the delta-BMI (dBMI), defined as: dBMI = (iBMI – BMI) / Height (in meters)
This index normalizes the differential between iBMI and BMI by the subject's height, allowing consistent comparison across body sizes. It was conceptualized as a continuous, algebraic surrogate for visceral fat predominance. Additionally, a visual metric, Graphical Risk Distance (GRD) was proposed, calculated as the vertical distance between a subject's data point and the EPL on the iBMI–BMI scatterplot. Mathematically, GRD was defined as the difference between the iBMI–BMI intercept and the iBMI–EPL intercept for a given BMI.

Validation and ROC Analysis:
Receiver Operating Characteristic (ROC) analysis was conducted to evaluate the predictive performance of GRD and dBMI against established metabolic risk markers. HOMA1-IR >1.7 was used as the primary benchmark for insulin resistance. Additional ROC models were developed using FPG, FPI, HbA1c, HOMA1-B, and GRD. Visceral fat measured by both bioelectrical impedance and DEXA (in grams) was also assessed in relation to GRD and dBMI. For binary classification in ROC analyses, the following cut-off values were applied based on clinical convention or median distribution: HOMA-IR >1.7 (insulin resistance), BEA-derived visceral fat >10 units, dBMI ≥15, GRD ≥0, HOMA-B ≥90, fasting plasma insulin ≥12 µIU/mL, fasting plasma glucose ≥100 mg/dL, and HbA1c ≥5.7%

Ethical Considerations:
This study involved a retrospective analysis of anonymized clinical data collected during routine care. No intervention or randomization was performed, and all patients had provided informed consent for use of their clinical records in academic and quality improvement activities. In accordance with national ethical guidelines, a waiver was duly given by the ethics committee of Poona Hospital & Research Centre, Pune, India.

Results

Metabolic Clustering and Profiles:
Unsupervised K-means clustering (k=3) identified three distinct metabolic phenotypes within the full dataset (n=331), visualized using principal component analysis (Figure 1). The unhealthy cluster (n=27; 8.2%) showed markedly elevated fasting plasma glucose (FPG, mean: 250.1 mg/dL), significantly higher than the healthy cluster (n=187; 56.7%; mean FPG: 110.5 mg/dL; $p = 1.6 \times 10^{-11}$), validating the clustering approach.
For risk stratification, we focused on a non-diabetic subset (n=208), excluding subjects with FPG >125 mg/dL or HbA1c >6.4%. This ensured an evaluation of early metabolic deviations prior to the onset of overt diabetes, where insulin and visceral fat markers are not yet significantly attenuated by disease progression or pharmacotherapy.

Visualizing the iBMI–BMI Relationship (Panel A):
Figure 2, Panel A, depicts a scatterplot of iBMI vs. BMI in the non-diabetic subgroup, with a linear regression line superimposed (iBMI = 2.49 × BMI – 23.27). This regression line, the Equipoise Line (EPL), serves as a theoretical boundary balancing subcutaneous (SAT) and visceral adiposity (VAT). Upward deviation from the EPL is interpreted as VAT predominance, while downward shift reflects relatively higher height or peripheral mass (e.g., gluteofemoral fat or muscle).

Diagnostic Accuracy of dBMI and GRD (Panels B, C, D):
Panels B through D present ROC curves assessing the diagnostic performance of GRD and dBMI, defined as (iBMI – BMI)/Height in meters) in predicting insulin resistance, operationalized as HOMA1-IR >1.7. Panel B (Glycemic Markers vs HOMA1-IR)
demonstrated moderate-to-strong predictive utility. (dBMI (AUC = 0.81) and GRD (AUC = 0.67)). dBMI performance was comparable to insulin-derived indices: FPI (AUC = 1.0), HOMA-B (0.89), FPG (0.74), and HbA1c (0.63). Panel C (Bioimpedance–Derived VF vs HOMA1-IR): BEA–VF (AUC = 0.80), dBMI (0.79), and GRD (0.71) all tracked insulin resistance well, despite being insulin-free metrics. Panel D (DEXA–Derived VF vs HOMA1-IR): In the DEXA subset (n=67), dBMI (AUC = 0.79) performed similarly to DEXA-VF itself (AUC = 0.71), supporting dBMI as a valid proxy for central adiposity.

Concordance Between dBMI and GRD (Panel E):
Panel E illustrates the correlation between dBMI and GRD, revealing a strong linear association: “dBMI = 14.78 + 0.68 × GRD, R^2 = 0.436”
The tight clustering around the regression line and 95% prediction interval band suggest that dBMI and GRD are convergent measures—one algebraic, the other geometric—capturing the same underlying risk gradient.

Nomogram Development and Risk Zoning (Panel F):
Panel F presents the iBMI–BMI nomogram, visually coded with risk zones derived from vertical distance from the EPL (the GRD):
- Low Risk: GRD < 0
- Minimal Risk: GRD 0 to +10
- Moderate Risk: GRD +10 to +20.5
- High Risk: GRD > +20.5

This visual framework enables intuitive risk classification without requiring explicit computation of dBMI. Clinicians can simply locate a data point on the nomogram to estimate central adiposity risk.

Discussion

The rationale for redefining obesity indices arises from longstanding limitations of the BMI, which does not account for WC, a key surrogate for visceral adiposity and fails to differentiate between lean and fat mass (Ashwell et al., 2012; Gallagher et al., 1996). Consequently, muscular individuals or those with predominantly gluteofemoral (peripheral) fat distribution are often misclassified. Ethnic-specific biases, such as the “Y-Y paradox” observed in South Asians, where metabolic risk is disproportionately high at lower BMI values, further limit its utility (Yajnik et al., 2004).

To overcome these shortcomings, we formulated the Improvised BMI (iBMI), defined as (Weight × WC) / Height. This composite index integrates both total body mass

and central adiposity in a height-adjusted manner. Unlike other indices such as Waist-to-Height Ratio (WtHtR), A Body Shape Index (ABSI) (Krakauer et al., 2012), and Body Roundness Index (BRI) (Thomas et al., 2013), iBMI strikes a pragmatic balance between biological accuracy and computational simplicity. Its design aligns with recent recommendations from the Lancet Commission on Obesity, which advocates for shifting from BMI-centric models to metabolically informed definitions (Rubino et al., 2023).

In the Asian population, a BMI threshold of 23 kg/m² typically marks the upper limit of normal adiposity. Beyond this point, accumulation of adipose tissue begins, encompassing both subcutaneous (SAT) and visceral fat (VAT). BMI is more reflective of SAT, while iBMI, incorporating WC, represents both SAT and VAT. Therefore, the difference between total adiposity (iBMI) and SAT (approximated by BMI) serves as a proxy for VAT. This difference corrected for height, termed differential BMI (dBMI), conceptually mirrors the estimation model used by CoreScan® in dual-energy X-ray absorptiometry (DEXA) to quantify visceral fat, as validated by imaging studies comparing DEXA with MRI (Ruano et al., 2025).

To normalize this difference for body size, we derived a novel height-adjusted index called the delta-BMI (dBMI), defined as:

$$dBMI = (iBMI - BMI) / \text{Height (in meters)}$$

This construct captures excess visceral adiposity across individuals of differing stature and was evaluated along with GRD for metabolic risk prediction. dBMI thus serves as a differential risk amplifier, quantifying the disproportion between central and generalized adiposity. It captures phenotypes like Metabolically Unhealthy Normal Weight (MUHW) and Metabolically Healthy Obese (MHO), often missed by traditional BMI. Stratifying dBMI into risk zones such as Low, Moderate, High and Very High provides a continuous and dynamic framework for metabolic risk tracking, especially in populations with heterogeneous body compositions.

The iBMI basal zone, extending up to the BMI threshold of 23 (i.e., ~35 kg·m/m for Indian males), accommodates muscular or pear-shaped individuals who would otherwise be over-diagnosed. Superimposing dBMI risk zones immediately above this baseline effectively transforms iBMI from a descriptive anthropometric measure into a clinically actionable risk prediction tool.

We developed a two-dimensional nomogram plotting iBMI against BMI, with superimposed dBMI iso-contour lines, to enable practical implementation. The central regression line—termed the Fat Equipoise Line (EPL)—was derived from the non-diabetic subset (n=208) and represents a physiological balance between waist circumference and height, assuming proportional contributions from BMI and WC. Vertical deviation from this line provides insight into adipose distribution: upward shifts indicate visceral adipose tissue (VAT) predominance, while downward deviations suggest greater subcutaneous adipose tissue (SAT) or peripheral mass contribution. The overlay of real-world data onto this nomogram confirmed that dBMI

zones effectively classify individuals into metabolically distinct phenotypes. Based on the distribution of residuals, a standard deviation of ±6.96 kg·m was observed, enabling construction of physiologically meaningful risk zones. Data points exceeding +1 SD above the EPL reflect elevated central adiposity and insulin resistance, aligning with the Metabolically Unhealthy Obese (MUHO) phenotype. In contrast, individuals falling below −1 SD display lower visceral fat burden despite comparable BMI values, consistent with the Metabolically Healthy Obese (MHO) profile. This visual stratification framework enhances interpretability, preserves quantitative accuracy, and mirrors established trajectories of insulin-independent risk accumulation—rendering it analogous in clinical utility to pediatric growth charts.

Figures 2B, C & D further validate iBMI as a waist-derived marker by demonstrating a strong linear correlation with visceral fat. ROC analysis reinforces the utility of dBMI, with an AUC of 0.81—comparable to HOMA-B (0.89) and outperforming HbA1c (0.63), fasting plasma glucose (0.74), and even BEA visceral fat measures (0.80). These results are consistent with the Korean Cancer Prevention Study, which identified a J-shaped curve between fasting glucose and cardiovascular risk, even within the normoglycemic range (Park et al., 2013).

Moreover, a recent Chinese study evaluating four visceral adiposity indices (LAP, CVAI, CMI, BRI) found that all correlated with prediabetes and diabetes, with LAP yielding the highest AUC (0.726) (Zhao et al., 2024). Notably, dBMI outperformed LAP in our cohort, suggesting it may offer a more integrated surrogate for VAT-related risk.

DEXA-Based Validation of dBMI:
To externally validate dBMI as a surrogate marker for visceral adiposity, we analyzed a subset of 67 participants who underwent body composition assessment via dual-energy X-ray absorptiometry (DEXA). dBMI demonstrated high discriminative accuracy for elevated visceral adipose tissue mass, yielding an AUC of 0.79 and outperforming glycemic indices such as HbA1c (AUC: 0.63). Additionally, DEXA-measured VAT correlated significantly with insulin resistance, with AUCs of 0.79 for HOMA1-IR. These findings indicate that dBMI captures metabolically relevant central adiposity with a precision approaching that of imaging standards. The strong concordance between anthropometric estimates and imaging-derived VAT reinforces the physiological validity of the iBMI–dBMI framework, and supports its use as a practical, scalable tool for risk stratification in clinical environments where such sophisticated imaging facility is not readily available.

Figure 2E demonstrates a significant linear relationship between Graphical Risk Distance (GRD) and the delta-BMI (dBMI), reinforcing the conceptual congruence between these two surrogate markers of visceral adiposity. The GRD, calculated visually as the vertical distance from the iBMI–BMI regression line, closely aligns with dBMI, which is analytically derived from the same anthropometric inputs. The observed regression equation indicates that for every unit increase in GRD, dBMI

increases by approximately 0.52 units, with an intercept around 15. This supports the premise that GRD serves as a visual analog to dBMI. The inclusion of a 95% prediction interval captures the expected inter-individual variation in the GRD–dBMI relationship, enhancing clinical interpretability. The moderate coefficient of determination ($R^2 = 0.436$) reflects physiological variability and reinforces the importance of incorporating both analytical and visual tools when assessing early adiposity-related risk.

Insulin resistance also carries a significant hereditary component. At-risk individuals may display early-onset metabolic dysfunction at lower iBMI levels. In our nomogram, such individuals appear above the EPL, highlighting both inherited and acquired vulnerability. Those with disproportionately high VAT also cluster above the EPL, reinforcing the association with MUHO.

Figure 2F relies on a data-derived regression trendline with ±1 SD bounds, enabling visual identification of metabolic divergence. This design improves both readability and diagnostic precision. Given that insulin resistance and β-cell dysfunction precede diabetes by years (Brunner et al., 2014; Holman et al., 2008), early identification tools are invaluable. iBMI and dBMI are well-positioned to meet this need. They are height-neutral, intuitive, and easily computable qualities that lend themselves well to low-resource settings, where biochemical or imaging infrastructure may be limited.

To operationalize iBMI as a waist-adjusted alternative to BMI, we developed a zone-based classification system anchored on the Fat Equipoise Line (EPL) derived from the iBMI–BMI regression in the non-diabetic population. The vertical intercept of each subject's iBMI above or below the EPL was used to compute the Graphical Risk Distance (GRD), which served as a continuous proxy for visceral adiposity. Based on the distribution of GRD, we defined iBMI zones by translating these intercept ranges into categorical thresholds: **<**26 (Underweight), 26–35 (Normal Weight), 36–40 (Overweight), 41–50 (Obesity Class I), 51–60 (Obesity Class II), and **>**60 (Obesity Class III). These zones were visually encoded in the iBMI–BMI nomogram and validated against metabolic markers and ROC-derived performance. By using GRD relative to the EPL as a physiologic axis, this framework ensures that classification reflects actual fat distribution rather than generalized body mass, offering a more accurate assessment of metabolic risk.

The normal reference iBMI value (35 kg·cm/cm) for Indian males was derived using population anthropometric data (Majumder, 2014) and the "mean + 1 SD" method. This threshold demarcates "non-obese" individuals, allowing us to compute a simple Obesity Index by comparing test values to this reference. Together, iBMI, dBMI, and their nomogram provide a physiologically coherent, scalable, and clinically meaningful platform for personalized obesity risk stratification.

In summary, this study introduces and validates two novel anthropometric indices—Improvised BMI (iBMI) and delta-BMI (dBMI), that overcome key limitations of

conventional BMI by incorporating waist circumference and height in a physiologically congruent manner. iBMI offers an intuitive, waist-based estimate of total and central adiposity, while dBMI, derived as the height-adjusted difference between iBMI and BMI, serves as a scalable surrogate for visceral fat burden. Both metrics demonstrated strong correlation with insulin resistance and visceral adiposity, comparable to standard biochemical markers and imaging-based assessments. Importantly, the graphical counterpart, Graphical Risk Distance (GRD), provides a visually interpretable analog to dBMI, enabling clinicians to stratify risk directly from the iBMI–BMI nomogram. The Fat Equipoise Line (EPL), derived from the non-diabetic population, anchors this visual framework and facilitates individualized risk zone classification. Collectively, iBMI, dBMI, and GRD constitute a coherent and accessible toolset for early identification of metabolic risk, particularly suited to low-resource settings or preclinical screening. Their integration into routine anthropometric assessment may enhance precision in obesity classification and inform more personalized interventions.

References

1. Quetelet A. *A Treatise on Man and the Development of His Faculties*. 1835.
2. Shah RV, Murthy VL, Abbasi SA, et al. Visceral adiposity and the risk of metabolic syndrome across body mass index: the MESA Study. *JACC Cardiovasc Imaging*. 2014;7(12):1221–1235.
3. Yajnik CS, Yudkin JS. The Y-Y paradox. *Lancet*. 2004;363(9403):163.
4. Rubino F, Puhl RM, Cummings DE, et al. The Lancet Commission on the definition and diagnosis of clinical obesity. *Lancet*. 2023;402(10403):965–1022.
5. Matthews DR, Hosker JP, Rudenski AS, Naylor BA, Treacher DF, Turner RC. Homeostasis model assessment: insulin resistance and beta-cell function from fasting plasma glucose and insulin concentrations in man. *Diabetologia*. 1985;28(7):412–419.
6. Krakauer NY, Krakauer JC. A new body shape index predicts mortality hazard independently of body mass index. *PLoS One*. 2012;7(7):e39504.
7. Thomas DM, Bredlau C, Bosy-Westphal A, et al. Relationships between body roundness with body fat and visceral adipose tissue emerging from a new geometrical model. *Obesity (Silver Spring)*. 2013;21(11):2264–2271.
8. Ashwell M, Gunn P, Gibson S. Waist-to-height ratio is a better screening tool than waist circumference and BMI for adult cardiometabolic risk factors: systematic review and meta-analysis. *Obes Rev*. 2012;13(3):275–286.

9. Majumder J. Anthropometric dimensions among Indian males — A principal component analysis. *Euras J Anthropol*. 2014;5(2):54–62.

10. Ruano GR, et al. Abdominal obesity and cardiometabolic risk markers: A comparative analysis of waist circumference, dual-energy X-ray absorptiometry, and magnetic resonance imaging techniques. *Nutr Metab Cardiovasc Dis*. 2025;35(3):103801.

11. Brunner EJ, Kivimäki M, Witte DR, et al. Adiposity, obesity, and risk of type 2 diabetes: findings from the Whitehall II Study. *Lancet Diabetes Endocrinol*. 2014;2(10):795–804.

12. Holman RR, Paul SK, Bethel MA, Matthews DR, Neil HA. 10-year follow-up of intensive glucose control in type 2 diabetes. *N Engl J Med*. 2008;359(15):1577–1589.

13. Park C, Guallar E, Linton JA, et al. Fasting glucose level and the risk of incident atherosclerotic cardiovascular diseases. *Diabetes Care*. 2013;36(7):1988–1993.

14. Zhao Q, Du Y, Liu M, et al. Comparison of four visceral obesity indices in identifying the risk of prediabetes and diabetes in Chinese middle-aged and elderly people. *BMC Endocr Disord*. 2024;24(1):25. doi:10.1186/s12902-024-01718-x

15. Indian Council of Medical Research (ICMR). *National Ethical Guidelines for Biomedical and Health Research Involving Human Participants*. New Delhi: ICMR; 2017. Available from: https://ethics.ncdirindia.org//asset/pdf/ICMR_National_Ethical_Guidelines_2017.pdf

Figure 1. Metabolic Clustering via PCA Projection: Unsupervised K-means clustering (k=3) was applied to fasting glucose, fasting insulin, and visceral fat (VF) data, and visualized via principal component analysis (PCA). The resulting plot identifies three distinct metabolic clusters, labeled Healthy, Intermediate, and Unhealthy. The separation along PC1 and PC2 reflects the dominant variance associated with metabolic risk parameters.

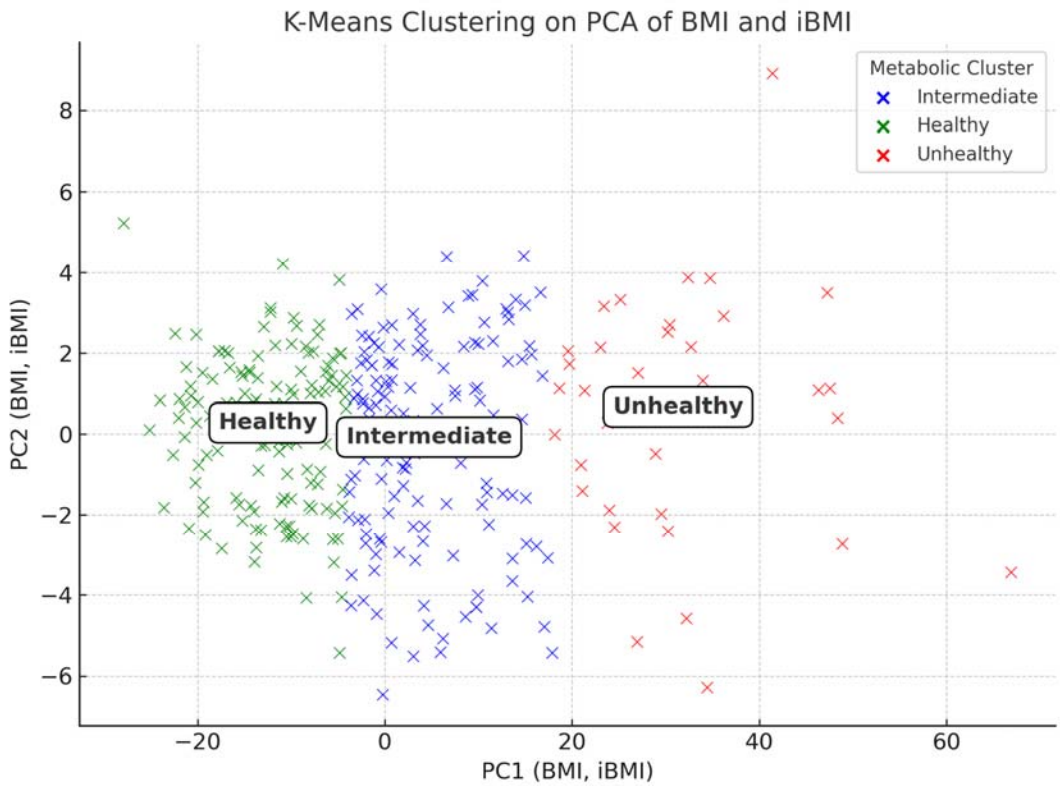
K-Means Clustering on PCA of BMI and iBMI
Metabolic Cluster
Intermediate
Healthy
Unhealthy
Healthy
Intermediate
Unhealthy
PC2 (BMI, iBMI)
PC1 (BMI, iBMI)
8
6
4
2
0
−2
−4
−6
−20
0
20
40
60

Figure 2. Composite 6-Panel Visualization of Key Study Findings:
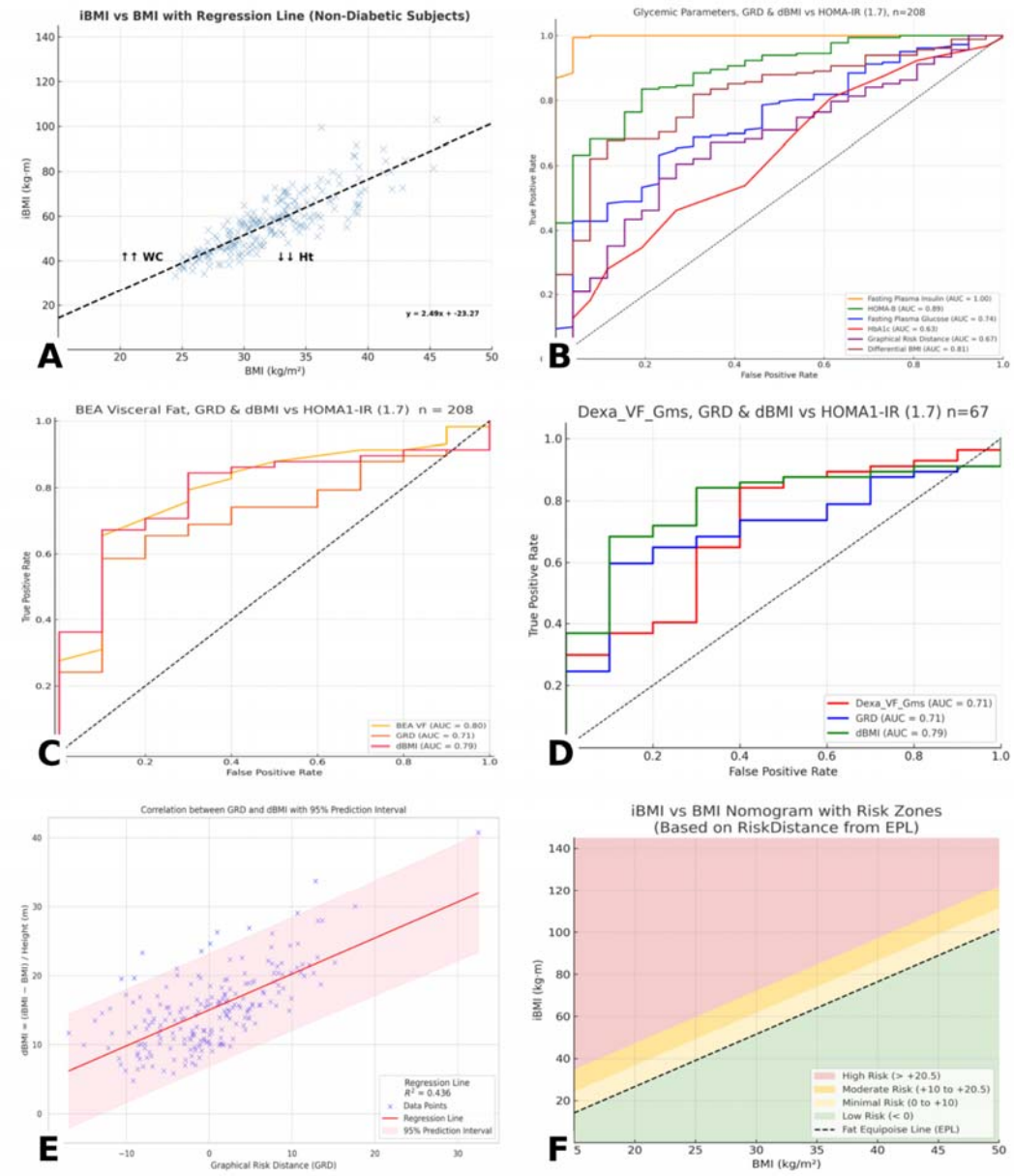
A. iBMI vs BMI in non-diabetic subgroup (n=208) with regression-based Fat Equipoise Line (EPL).
B. ROC curves comparing GRD, dBMI, and biochemical markers (FPG, HbA1c, FPI, HOMA-B) vs HOMA1-IR >1.7.
C. ROC curves comparing GRD, dBMI, and BEA-derived visceral fat vs HOMA1-IR.
D. ROC curves comparing GRD, dBMI, and DEXA-derived VAT vs HOMA1-IR.
E. Linear regression plot between dBMI and GRD with $R^2 = 0.436$ and 95% prediction interval.
F. Final nomogram (iBMI vs BMI) with superimposed GRD risk zones (Low, Moderate, High).